



Supplement of

Captive Aerosol Growth and Evolution (CAGE) chamber system to investigate particle growth due to secondary aerosol formation

Candice L. Sirmollo et al.

Correspondence to: Don R. Collins (donc@ucr.edu)

The copyright of individual parts of the supplement might differ from the article licence.

Supplement

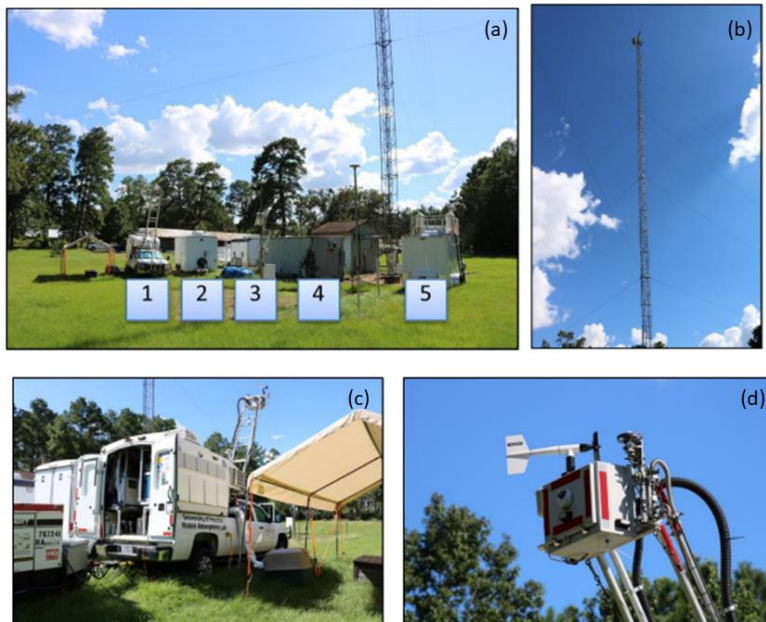


Figure S1. First generation CAGE chambers, which were referred to as QUALITY chambers in some publications.

5



Figure S2. Close-up photo of a CAGE chamber highlighting the overall clarity.



10 Figure S3. Pictures of MAQL instrumentation and research trailer setup at JSF during field campaign. (a): JSF sampling site within an open clearing of the forest facing southwest, where the following are shown from left to right and are numbered from 1 to 5: (1) University of Houston/Rice University MAQL, (2) Sandia National Laboratories trailer, (3) Texas A&M University trailer, (4) University of Houston/Rice University secondary trailer, and (5) Baylor University trailer, (b): TCEQ CAMPS698 tower located at the site from which wind speed and wind direction data are collected, (c): MAQL showing access to the rear instrumentation bed, and (d): Trace

15

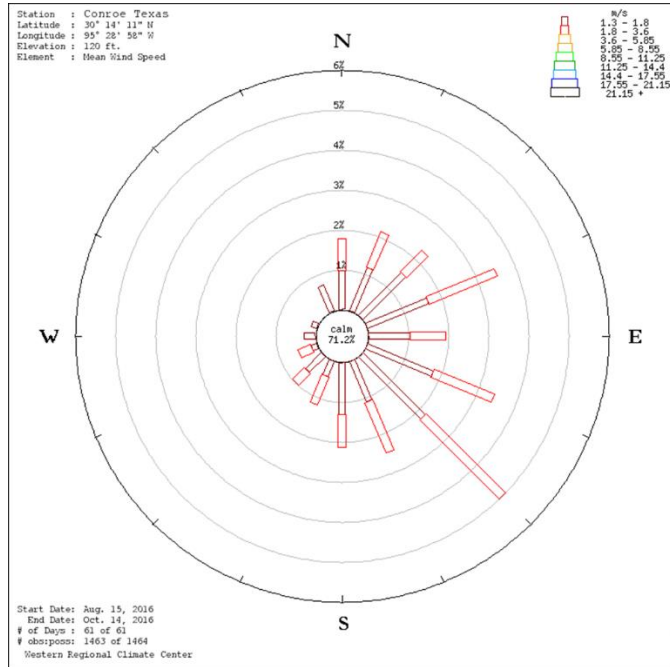


Figure S4. Wind rose calculated for the period of the field study (August 15 – October 14, 2016) at the nearby Conroe airport. Courtesy of the Western Regional Climate Center (wrcc.dri.edu).

20

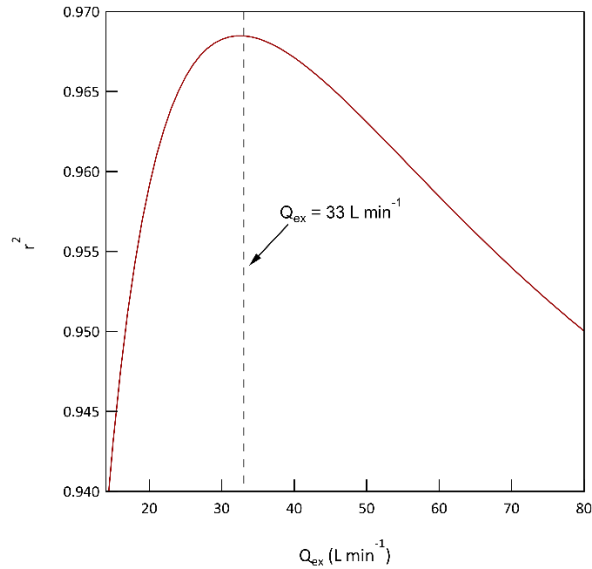


Figure S5. Relationship of the correlation between time series of NO_y concentration i) measured in the chambers and ii) determined from the ambient measurements assuming the chambers can be modeled as CSTRs with exchange flow rate Q_{ex}. The Q_{ex} used for all subsequent calculations is that at which r² was highest. The average of the results for Chambers A and B is shown.

25

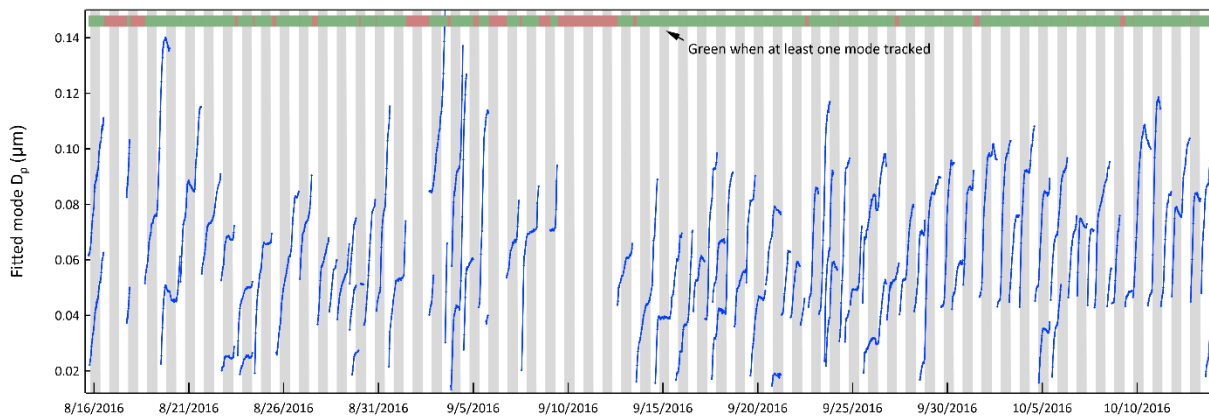


Figure S6. Time series of lognormal fit diameter to all modes tracked during the 2016 study. The color bar towards the top of the graph indicates the periods during which at least one mode was tracked and growth rate could be determined. The gap from 9/9/2016 to 9/12/2016 was the three-day gas-phase comparison experiment discussed in Sect. 4.1.

30

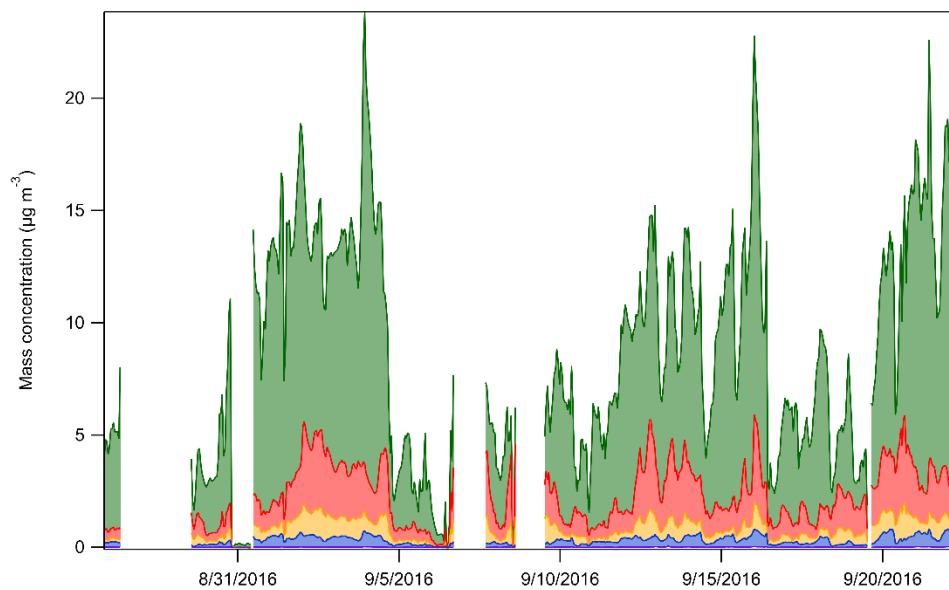


Figure S7. Sub-1 μm non-refractory composition of ambient aerosol measured with an HR-ToF-AMS. The colors indicate the following species: green = organics, red = sulfates, yellow = ammonium, and blue = nitrates.

35

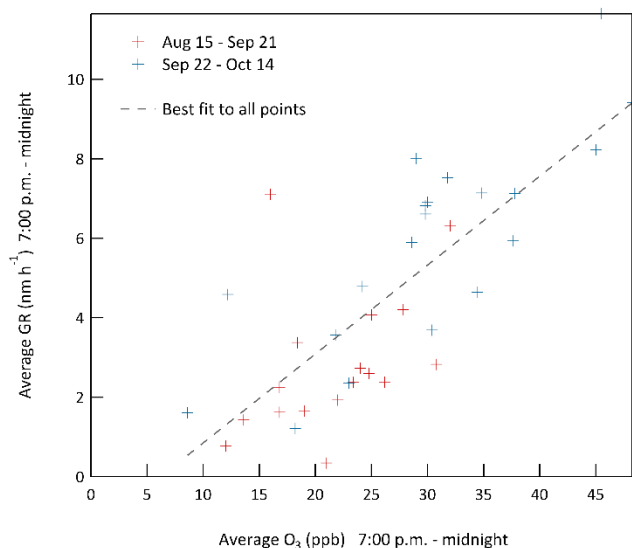


Figure S8. Relationship between the early evening average growth rate and average O₃ mixing ratio. The correlation between the two and the general increase in both during the fall suggests that some of the increased nighttime particle growth towards the end of the project was associated with increased O₃.

40

Table S1. Reactions included in the CSTR-0D model

Reaction	Rate coefficient (cm ³ s ⁻¹ unless stated otherwise)	Notes
NO + O ₃ → NO ₂ + O ₂	1.40 x 10 ⁻¹² exp(-1310/T)	
NO ₂ + O ₃ → NO ₃ + O ₂	1.40 x 10 ⁻¹² exp(-2470/T)	
NO ₂ + NO ₃ (+ M) → N ₂ O ₅	1.9 x 10 ⁻¹² (T/300) ^{0.2}	High pressure limit rate constant and expression
N ₂ O ₅ + M → NO ₂ + NO ₃	1.30 x 10 ⁻³ (T/300) ^{-3.5} exp(-11000/T)	
NO ₃ + NO → 2NO ₂	1.80 x 10 ⁻¹¹ exp(110/T)	
OH + NO (+ M) → HONO	1.50 x 10 ⁻¹¹ (T/300) ^{-0.5}	High pressure limit rate constant and expression
OH + NO ₂ (+ M) → HNO ₃	2.40 x 10 ⁻¹¹ (T/300) ^{-1.3}	High pressure limit rate constant and expression
NO ₃ + RO ₂ → NO ₂	2.00 x 10 ⁻¹²	
RO ₂ + RO ₂ → products	2.00 x 10 ⁻¹²	
OH + acetaldehyde → RO ₂	5.55 x 10 ⁻¹² exp(287/T)	
<i>Photolysis reactions</i>		
NO ₂ + hv → NO + O ₃	J _{NO2}	Calculated assuming photostationary state for ambient NO, NO ₂ , and O ₃ concentrations
NO ₃ + hv → 0.12NO + 0.88NO ₂ + 0.88O ₃	J _{NO3}	Calculated from measured spectral intensity
O ₃ + hv → 0.3OH + O ₃	J _{O1D}	Calculated from measured spectral intensity. Assumes 15% of O(¹ D) produced reacts with H ₂ O

		to form OH·. O ₃ is conserved because any shift this would cause would be captured in the estimated J _{NO₂} .
HONO + hv → OH· + NO	J _{HONO}	Calculated from measured spectral intensity
<i>Secondary aerosol forming reactions</i>		
OH· + α-pinene → RO ₂ ·	2.54 x 10 ⁻¹¹ exp(410/T)	
OH· + β-pinene → RO ₂ ·	1.21 x 10 ⁻¹¹ exp(444/T)	
OH· + isoprene → 0.6RO ₂ · + 0.4MVK+MACR	2.38 x 10 ⁻¹¹ exp(357/T)	
OH· + toluene → RO ₂ ·	1.81 x 10 ⁻¹² exp(280/T)	
OH· + SO ₂ → SO ₄	1.50 x 10 ⁻¹²	
O ₃ + α-pinene → RO ₂ ·	6.30 x 10 ⁻¹⁶ exp(-580/T)	
O ₃ + β-pinene → RO ₂ ·	1.20 x 10 ⁻¹⁵ exp(-1300/T)	
O ₃ + isoprene → 0.6RO ₂ · + 0.4MVK+MACR	1.03 x 10 ⁻¹⁴ exp(-1995/T)	
NO ₃ · + α-pinene → RO ₂ · + 0.8NO ₂	1.20 x 10 ⁻¹² exp(490/T)	
NO ₃ · + β-pinene → RO ₂ · + 0.3NO ₂	2.50 x 10 ⁻¹²	
NO ₃ · + isoprene → 0.95RO ₂ · + 0.3NO ₂ + 0.05MVK+MACR	3.15 x 10 ⁻¹² exp (-450/T)	
<i>Heterogeneous reactions</i>		
N ₂ O ₅ + H ₂ O(ℓ) → 2HNO ₃	2.67 x 10 ⁻⁷ x S (μm ² cm ⁻³) ³⁾	Aerosol surface area, S, assumed to be 100 μm ² cm ⁻³
<i>Tuning reactions</i>		
O ₃ + wall → 0.65acetaldehyde + 0.12acetone	1.00 x 10 ⁻⁴ s ⁻¹ for A 0.70 x 10 ⁻⁴ s ⁻¹ for B	Used to match observed O ₃ loss and acetaldehyde and acetone production. Wall “concentration” dependent upon solar intensity to adjust for increase in contact frequency with increased convective mixing.
OH· + X →	2 s ⁻¹	Used to produce reasonable daily peak OH·. Partially constrained by daytime difference between chamber and ambient isoprene resulting from reaction with OH·.
(N ₂ +O ₂) + wall → HONO	1.0 x 10 ⁷ s ⁻¹	Recognized radical source in Teflon® chambers. Partially constrained by pattern of daytime difference between chamber and ambient isoprene resulting from reaction with OH·.

- OH \cdot is conserved for all “OH \cdot + reactant \rightarrow ” reactions because an independent overall OH \cdot reactivity is assumed.
 - Species in parentheses involved in reaction but not needed for calculated rate.
- 45
- Chamber temperature assumed to be the same as ambient temperature.